Performance Investigation and Optimization of Perovskite/CIGS Tandem Solar Cell by Using SCAPS-1D Modeling and Simulation

Dinuka R Ratnasinghe
Faculty of Graduate Studies
University of Sri Jayewardenepura
Nugegoda, Sri Lanka.
dinuka@sjp.ac.lk

Nipuna L Adihetty
Faculty of Graduate Studies
University of Sri Jayewardenepura
Nugegoda, Sri Lanka.
nladhi@sjp.ac.lk

Muthuthanthrige L. C. Attygalle
Department of Physics
University of Sri Jayewardenepura
Nugegoda, Sri Lanka.
lattygalle@sci.sjp.ac.lk

Hasitha Mahabaduge
Department of Chemistry, Physics and Astronomy
Georgia College & State University
Milledgeville, USA
hasitha.mahabaduge@gcsu.edu

2021 Moratuwa Engineering Research Conference (MERCon) | 978-1-6654-3753-0/21/$31.00 ©2021 IEEE | DOI: 10.1109/MERCON52712.2021.9525755

***Abstract* — In the photovoltaic industry, perovskites that belong to the third generation are one of the most popular materials which give more promising results. The $CH_3NH_3PbI_3$ (Methylammonium Lead Iodide) also known as MAPI is one of the famous material which gives higher performances. The research work was focused on modeling a multi-junction device with a perovskite top cell and second generation bottom cell. These two cells were modeled and simulated under AM1.5G illumination and the final model of the tandem cell was optimized by considering the thicknesses of the absorber layers which is key to the performance. A surface defect layer (SDL) which previously proved buried homojunction was created at the CdS/CIGS interface. The existence of this layer increases the recombination at the homojunction. Therefore altering the properties of this layer was supposed to reduce the recombinations at the interface. The defect densities of the CdS/SDL and SDL/CIGS interfaces were analyzed and interpreted for all the possible outcomes. According to results, this tandem model showed 30.95% power conversion efficiency (PCE) with 1.82 V open-circuit voltage and 20.86 mA/cm^2 short circuit current at the 0.19–0.20 µm thickness of perovskite absorber. All the modelings and simulations were done by using the SCAPS-1D software.**

Keywords—Tandem, Perovskite, CIGS, SDL, Optimization, SCAPS-1D

I. INTRODUCTION

In the present day, multi-billion-dollar projects are running in the photovoltaic industry to overcome the existing non-renewable energy productions. But when considering the global energy demand, the contribution of solar cells is still negligible. Therefore, researchers are working on finding new solutions to enhance the performances of these Photovoltaic (PV) devices. When considering the three generations of solar cells [1, 2], the c-Si which belongs to the first generation is still dominating the PV industry. The second-generation a-Si, CdTe, and CIGS devices are producing cost-efficient products and it is still in second place. But due to the high trend and more promising results the third generation is becoming a more popular topic. With the approach of the multi junctional PV devices, researchers identified a clear path to reach Shockley & Queisser's detailed balanced limit [3]. The maximum theoretical efficiency for the tandem device is 47% under the unconcentrated AM1.5G spectrum [4, 5].

This research work is about computational modeling of a multijunction device and a simulation study by combining the third and second-generation PV devices. Here the third generation PV device was used as the top cell to harvest high-energy photons from the spectrum. This cell is supposed to absorb the energies under the wavelength of 300-800 nm. Especially the perovskite materials are also capable of absorbing high energies within the UV range. In the bottom cell configuration, a previously modeled thin-film structure was used to harvest low energies. The major goal of this research study is to optimize the multijunctional device to obtain the best efficient model. Therefore two areas were focused on optimizing which were thickness optimization of the top cell absorber and defect density alteration at the buried homojunction at the CdS/CIGS interface.

In order to find the photocurrent, the absorption coefficient of the materials which is an optical parameter should be estimated by using the following equation,

$$\alpha_c(\lambda) = \begin{cases} 0, \frac{hc}{\lambda} < E_g \\ \frac{B\lambda}{hc}\left(\frac{hc}{\lambda} - E_g\right)^{1/2}, \frac{hc}{\lambda} > E_g \end{cases} \quad (1)$$

where, α_c is absorption coefficients with respect to each material, h is Planck's constant, c is the speed of light, λ is the wavelength, B is a constant which depends on the effective masses and E_g is the bandgap of each material.

The photocurrent of each cell can be estimated by solving the Poisson, continuity and the photocurrent at the neutral zone can be estimated with carrier transport equations. Meanwhile, the photocurrent at the space charge region (SCR) can be estimated by using the following expression,

$$I_{ph} = \int_{\lambda_{min}}^{\lambda_{max}} I_d(\lambda) + I_b(\lambda) + I_e(\lambda) \quad (2)$$

where, I_{ph} is the generated photocurrent, λ_{min} is the lower bound of the wavelength, λ_{max} is the upper bound of the

University of Sri Jayewardenepura, Sri Lanka.

978-1-6654-3753-0/21/$31.00 ©2021 IEEE

wavelength and $I_d(\lambda)$, $I_b(\lambda)$, $I_e(\lambda)$ are the photocurrents generated at the depletion, base, and emitter regions as a function of wavelength.

Here the $I_d(\lambda)$, $I_b(\lambda)$, and $I_e(\lambda)$ are dependent on the quasi-neutral region lengths and the depletion widths extended to the emitter and absorber materials. Therefore the thickness of the emitter and the absorber materials are directly responsible for device efficiency [6].

Also, the minority carrier lifetime is related to the recombination times which has the following relation [7].

$$\frac{1}{\tau_n} = \frac{1}{\tau_b} + \frac{1}{\tau_s} + \frac{1}{\tau_{au}} \quad (3)$$

Where the τ_n, τ_b, τ_s, τ_{au} are respective to total recombination time bulk recombination time, surface recombination time, and the augur recombination time.

The τ_s has a relation with absorber material [7],

$$\frac{1}{\tau_s} = \frac{2S}{d_p} \quad (4)$$

$$S = V_{th}\sigma D_i \quad (5)$$

Where the d_p, V_{th}, σ, D_i are respective to the thickness of the absorber, carrier thermal velocity, capture coefficient, and the interface defect density.

II. Methodology

In this research study SCAPS-1D (one-dimensional solar cell capacitance simulator) software was used for all the simulations and modeling [8]. All the material data (electrical parameters) were extracted from previous research works [9-15]. In the simulation, the modeled device was tested under the AM1.5G spectrum [16]. Here the AM1.5G spectrum represents the direct and diffusion radiation of one-sun illumination. Here no concentration technique or filtering was used for the spectrum.

Here top cell of the tandem device is modeled with a perovskite material called 3D-MAPI (Three-dimensional Methylammonium Lead Iodide) [17], PEDOT:PSS (poly(3,4-ethylenedioxythiophene) polystyrene sulfonate), and PCBM ([6,6]-Phenyl-C61-butyric acid methyl ester) materials. The SnO_2 was used to create a Transparent Conducting Oxide (TCO) layer. The PCBM and PEDOT:PSS are acting as electron and hole transferring materials [18, 19]. In the perovskite material, shallow and amphoteric defects were created for SRH recombinations.

The bottom cell was modeled with second-generation materials such as CIGS, CdS, and ZnO materials. Additionally, an SDL was created at the CdS/CIGS interface [20]. The purpose of using the SDL layer is to study the properties of the homojunction at the surface of the bottom cell absorber.

It was previously shown that a homojunction exists at the surface of the bulk absorber [21-24]. The existence of the homojunction at the interface reduced the width of the SCR and this is causing higher recombinations at the junction. Therefore studying the properties of this homojunction is important. Here two interfaces; CdS/SDL and SDL/CIGS were analyzed to identify the influence of the interfacial defect densities. The SRH (Shockley-Read-Hall) recombination [25, 26] as known as recombination through defects was considered as the main recombination mechanism.

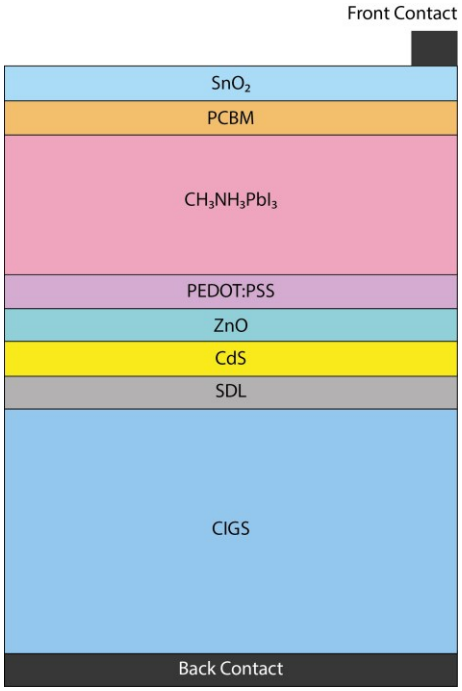

Fig. 1. The illustration of tandem cell configuration

The PEDOT:PSS/ZnO junction is working as a tunnel junction in the tandem configuration (Fig. 1). At this junction, the holes generated at the top cell recombines with the electrons come from the bottom cell. Mainly the thickness optimizations were carried out on absorber layers; MAPI and CIGS until achieving the current matching condition [27]. In the modeling, these two cells were separately created and simulated by using a SCAPS script. In this procedure, two artificial layers were created for each cell to concern partial absorptions. Fig. 2 represents the illustration of the two separate simulation models with artificial layers.

The two artificial layers were created according to the top and bottom cell configurations. The top cell was simulated with an artificial bottom layer and the bottom cell was simulated with an artificial top layer. These two artificial layers have the electrical properties of the top and bottom cells. This is a unique technique which using in SCAPS-1D multi-junction simulations.

Here the V_{oc} decreases with increasing perovskite absorber layer thickness. The voltage drop quite small compared to the current density variation. The J_{sc} and Efficiency of the top cell increase with the thickness of the Perovskite layer.

This simulation study was mainly focused on altering the key parameters, such as electrical properties and the thicknesses of absorber layers. Here, more importantly, the thickness variation of the top cell absorber is the key to the performance of the tandem cell (Fig. 3) and it has a high influence on bottom cell performance. The increment of the top cell absorber thickness creates a wider optical path and this will leads to higher photon absorption in the bulk material. Due to this phenomenon, the bottom cell absorbs less amount of photons, and therefore the efficiency of the bottom cell decreases. Fig. 4 shows the bottom cell

parameters variation with the thickness of the top cell absorber. Here the parameters; V_{oc}, J_{sc}, and Efficiency were decreased due to the thickening of the top cell absorber. These top and bottom cell shows contradictory J_{sc} variation. Due to the thickening of the Perovskite layer, the J_{sc} of both cells were closely coordinated at a certain point.

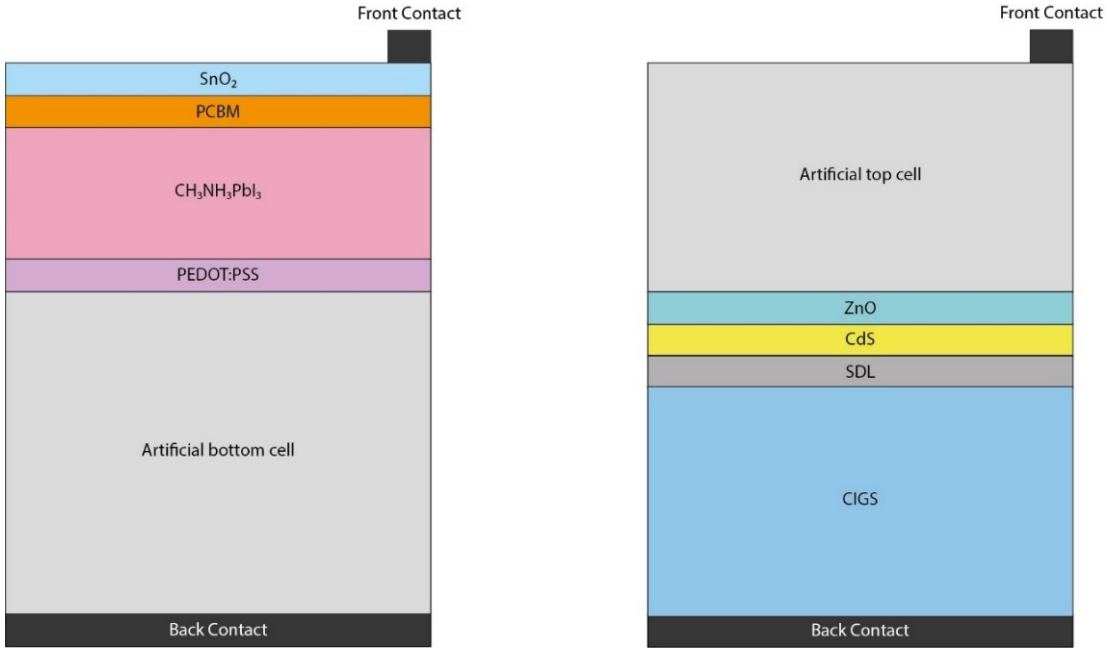

Fig. 2. Illustration of two simulation models with artificial layers.

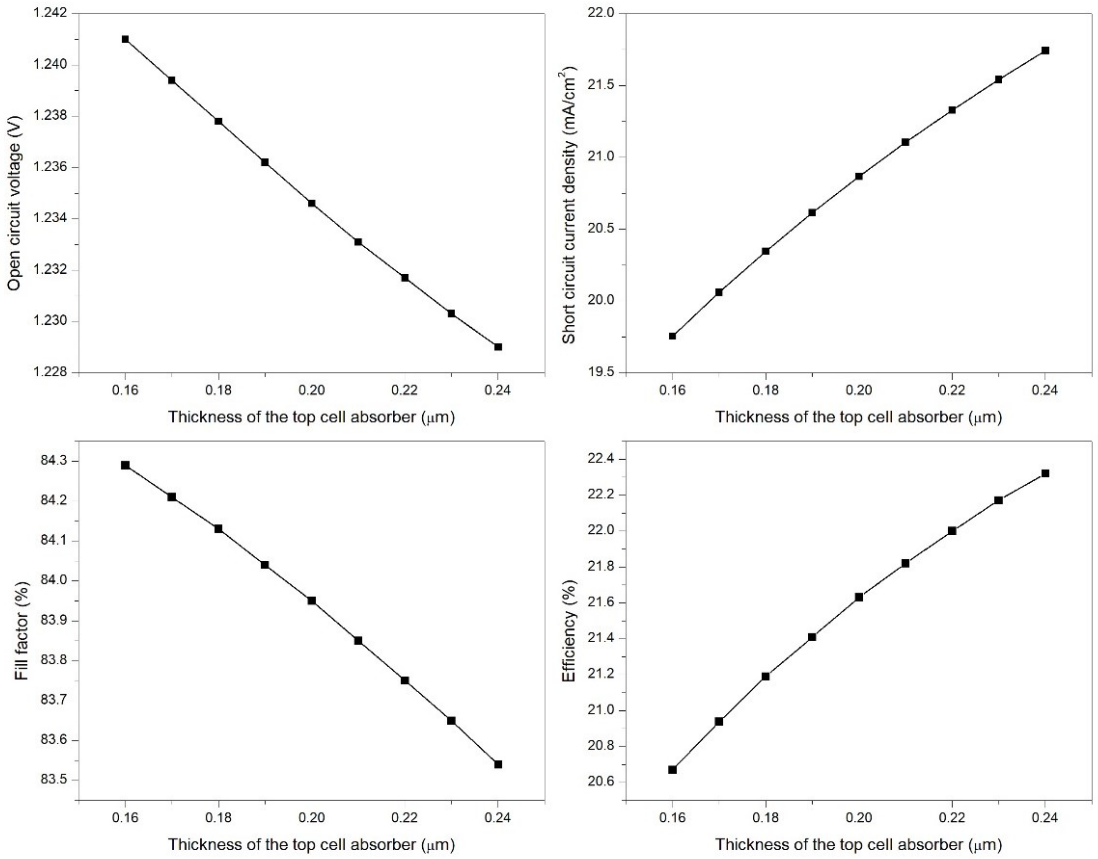

Fig. 3. Device parameter variation of the top cell with the thickness variation of the absorber layer

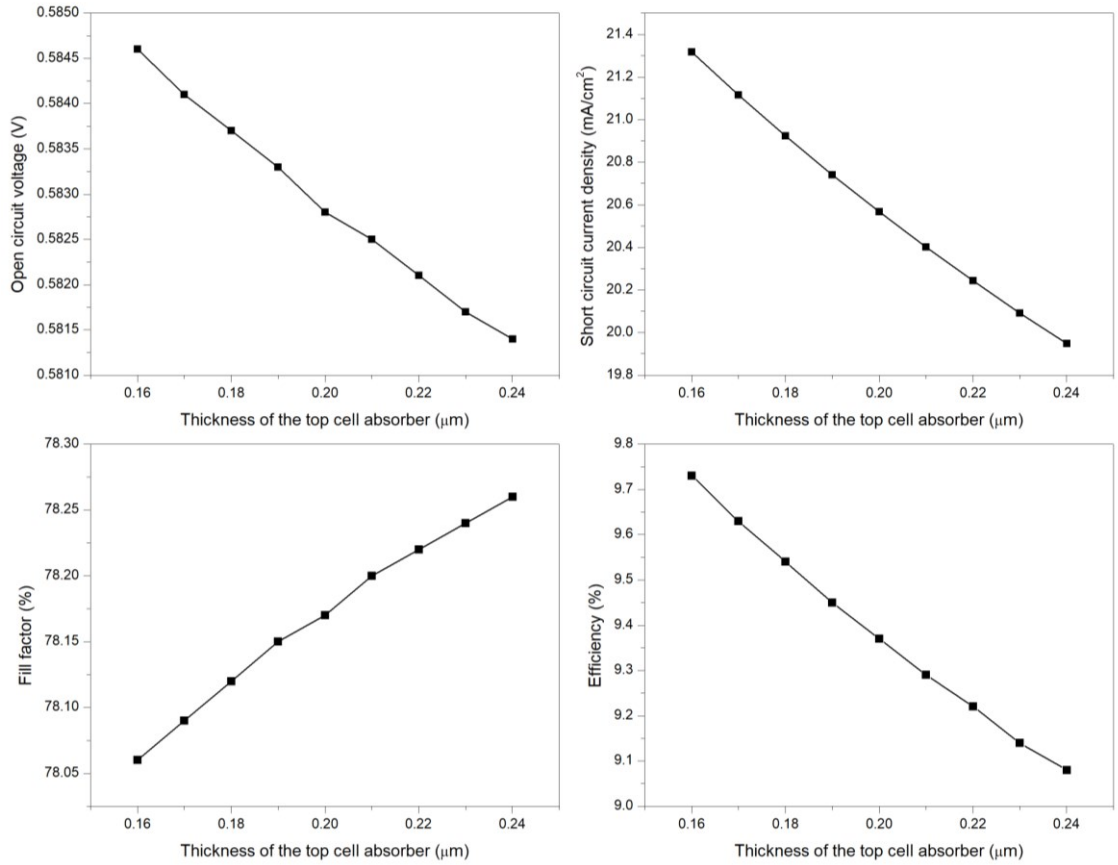

Fig. 4. Device parameter variation of the bottom cell with the thickness variation of the top cell absorber layer

This current matching condition can be observed in the 0.19–0.20 μm thickness range. More accurately the optimum condition can be obtained closer to 0.19 μm. In the simulation, the interval of the thickness variation of the top cell absorber was considered as 0.01 μm. the data points of Fig. 5 represent the obtained results and the exact point was identified by using numerical analysis.

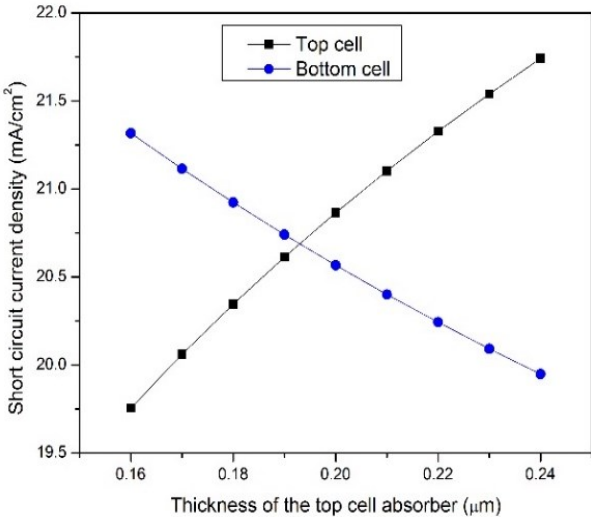

Fig. 5. Short circuit current density variation with the thickness of the top cell absorber

As described in the previous section the thicknesses were optimized to enhance the performance of the tandem device. Fig. 6 represent the JV characteristic curve and EQE curve of the top, bottom, and tandem devices. Here the top and bottom cells were optimized until obtaining the current matching condition. At the current matching condition, the optimum efficiency was observed

According to the EQE curves, the top cell showed the peak performance between the wavelength range of 300-800 nm as expected and the bottom cell showed between 600-1200 nm. Here 300–500 nm range is completely absorbed by the top cell.

The tandem structure was simulated under the AM1.5G spectrum and in the wavelength range of 300–1300 nm. According to the EQE curve the top cell performed under the wavelength range of 300–800 nm and the bottom cell performed under the wavelength range of 700-1200 nm. According to the results, the tandem cell showed an efficiency of 30.94% with 1.81 V open-circuit voltage and 20.86 mA/cm^2 short circuit current.

Fig. 8 shows the observed result of the defect density analysis of CdS/SDL and SDL/CIGS interfaces and here point defects were added to the CdS, SDL, and CIGS bulk materials.

Applying the SDL layer to the CdS/CIGS interface creates heterojunction with the CdS layer and homojunction with the CIGS absorber. Therefore, it creates a valance band offset at the edge of the absorber as shown in Fig. 7 (b). When altering the defects at the junction, SDL/CIGS interface show a higher influence of recombination compared to the CdS/SDL interface (Fig. 8).

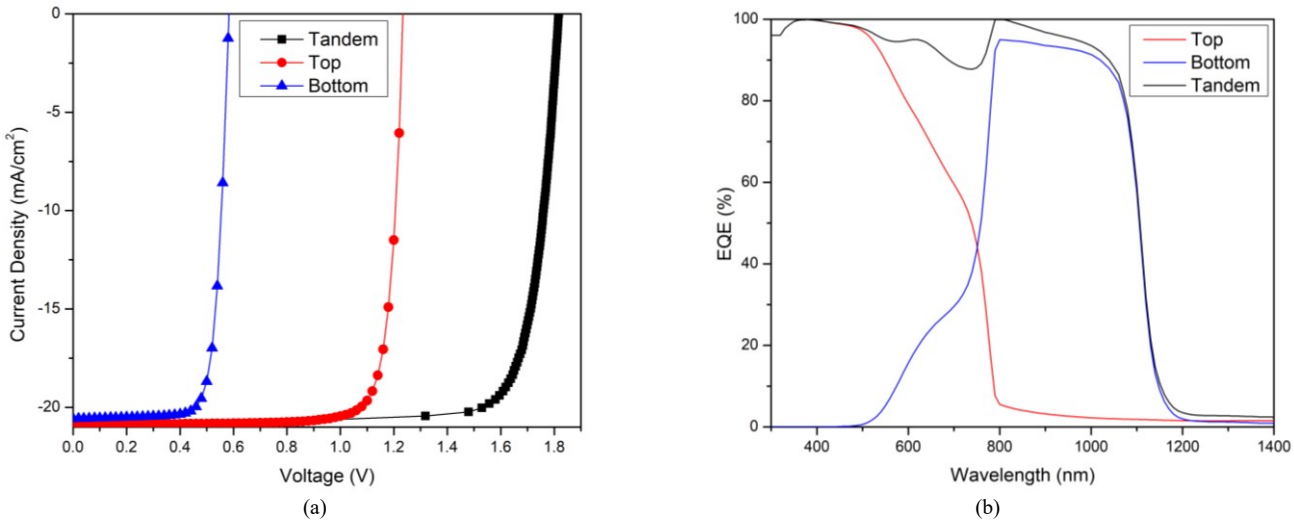

Fig. 6. IV characteristic curves (a) and EQE curves (b) of top, bottom, and tandem cells

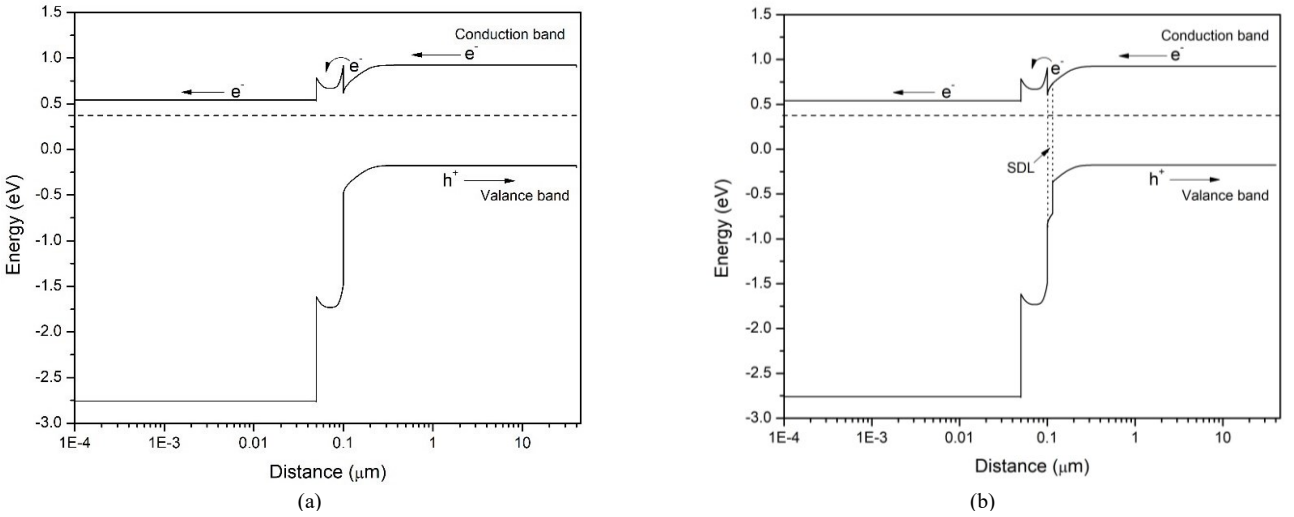

Fig. 7. Valance band offset modification (a) without SDL layer and (b) after applying SDL

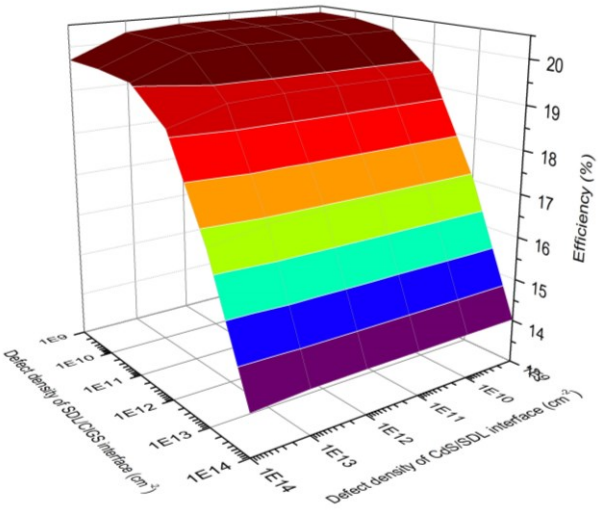

Fig. 8. The efficiency variation with the defect density alteration of the interfaces

An independent simulation of the bottom cell showed 20.38% efficiency with 0.63 V open-circuit voltage and 38.91 mA/cm^2 short circuit current density without the SDL. The bottom cell with SDL showed 20.32% efficiency with 0.63 V open-circuit voltage and 38.94 mA/cm^2 short circuit current density. Here introducing SDL increases the efficiency of the bottom cell by 0.06 %. But in the tandem operation, this efficiency increment was reduced to 0.03%. In this simulation, the interface defect density of both CdS/SDL and SDL/CIGS was selected as 1×10^{11} cm^{-2}.

III. Conclusions

This research work was conducted to model a tandem configuration by using perovskite and CIGS materials. The thickness optimization of the absorber layers was completed and the current matching condition was also obtained. Therefore this confirmed that the maximum efficiency can be obtained at the current matching condition of the tandem device which can be observed at the thickness range of 0.19–0.20 μm of perovskite absorber

According to the results of the defect density analysis, it can be concluded that the performance of the tandem device can be easily changed by altering the thickness of the top cell absorber and the defect density of the bottom cell SDL/CIGS interface. The defect concentration of the CdS/SDL interface can be varied on a large scale. But more importantly, the defect concentration of the SDL/CIGS interface should not exceed 1×10^{11} cm^{-2}. The existence of the homojunction at the surface of the bottom cell absorber decreases the performance, but altering the defect densities at the interfaces slightly increases the device performance. In the modeling, many assumptions were used, and fabricating the model is recommended to observe the real situation device configuration.

ACKNOWLEDGMENT

All the authors are pleased to acknowledge the two research grants; ASP/01/RE/SCI/2016/29 and MSTR/TRD/AGR/03/02/15 for funding this project. Also, we would like to deeply acknowledge the helpful discussions and the ideas given by Prof. Marc Burgelman about modeling the tandem structures using SCAPS-1D.

REFERENCES

[1] G. Conibeer, "Third-generation photovoltaics," *Materials today,* vol. 10, no. 11, pp. 42-50, 2007, doi: https://doi.org/10.1016/S1369-7021(07)70278-X.

[2] M. A. Green, "Third generation photovoltaics: Ultra-high conversion efficiency at low cost," *Progress in Photovoltaics: Research and Applications,* vol. 9, no. 2, pp. 123-135, 2001, doi: 10.1002/pip.360.

[3] W. Shockley and H. J. Queisser, "Detailed balance limit of efficiency of p-n junction solar cells," *Journal of applied physics,* vol. 32, no. 3, pp. 510-519, 1961, doi: https://doi.org/10.1063/1.1736034.

[4] N. N. Lal, Y. Dkhissi, W. Li, Q. Hou, Y. B. Cheng, and U. Bach, "Perovskite tandem solar cells," *Advanced Energy Materials,* vol. 7, no. 18, p. 1602761, 2017, doi: https://doi.org/10.1002/aenm.201602761.

[5] A. De Vos, "Detailed balance limit of the efficiency of tandem solar cells," *Journal of Physics D: Applied Physics,* vol. 13, no. 5, p. 839, 1980, doi: https://doi.org/10.1088/0022-3727/13/5/018.

[6] H. Ferhati and F. Djeffal, "An efficient analytical model for tandem solar cells," *Materials Research Express,* vol. 6, no. 7, p. 076424, 2019, doi: https://doi.org/10.1088/2053-1591/ab1596.

[7] M. Krichen and A. B. Arab, "Analytical study of a-Si: H/c-Si thin heterojunction solar cells with back surface field," *Journal of Computational Electronics,* vol. 15, no. 1, pp. 269-276, 2016, doi: https://doi.org/10.1007/s10825-015-0756-3.

[8] *SCAPS manual*, 8-4-2021 ed., 2016. [Online]. Available: https://users.elis.ugent.be/ELISgroups/solar/projects/scaps/SCAPS%20manual%20most%20recent.pdf. Accessed: May. 15, 2021.

[9] S. Adachi, *Optical constants of crystalline and amorphous semiconductors: numerical data and graphical information*. Springer Science & Business Media, 1999.

[10] Q. Wali, N. K. Elumalai, Y. Iqbal, A. Uddin, and R. Jose, "Tandem perovskite solar cells," *Renewable and Sustainable Energy Reviews,* vol. 84, pp. 89-110, 2018, doi: https://doi.org/10.1016/j.rser.2018.01.005.

[11] N. Khoshsirat, N. A. M. Yunus, M. N. Hamidon, S. Shafie, and N. Amin, "Analysis of absorber layer properties effect on CIGS solar cell performance using SCAPS," *Optik,* vol. 126, no. 7-8, pp. 681-686, 2015, doi: https://doi.org/10.1016/j.ijleo.2015.02.037.

[12] T. Erb, U. Zhokhavets, H. Hoppe, G. Gobsch, M. Al-Ibrahim, and O. Ambacher, "Absorption and crystallinity of poly (3-hexylthiophene)/fullerene blends in dependence on annealing temperature," *Thin Solid Films,* vol. 511, pp. 483-485, 2006, doi: https://doi.org/10.1016/j.tsf.2005.12.064.

[13] J. Hwang, D. Tanner, I. Schwendeman, and J. R. Reynolds, "Optical properties of nondegenerate ground-state polymers: Three dioxythiophene-based conjugated polymers," *Physical Review B,* vol. 67, no. 11, p. 115205, 2003, doi: https://doi.org/10.1103/PhysRevB.67.115205.

[14] L. J. Phillips *et al.*, "Dispersion relation data for methylammonium lead triiodide perovskite deposited on a (100) silicon wafer using a two-step vapour-phase reaction process," *Data in brief,* vol. 5, pp. 926-928, 2015, doi: https://doi.org/10.1016/j.dib.2015.10.026.

[15] M. Gloeckler, "Device physics of Cu (In, Ga) Se2 thin-film solar cells," Colorado State University, 2005.

[16] R. E. Bird, R. L. Hulstrom, and L. Lewis, "Terrestrial solar spectral data sets," *Solar energy,* vol. 30, no. 6, pp. 563-573, 1983, doi: https://doi.org/10.1016/0038-092X(83)90068-3.

[17] N. L. Adihetty, D. Ratnasinghe, M. Attygalle, N. Som, and P. Jha, "Numerical Modeling of Thin Film Solar Cell with Hybrid 3D/2D Organic-Inorganic Halide Perovskite under Low Light Conditions and AM 1.5 G Full Sun Spectrum," *INTERDISCIPLINARY APPROACHES IN SCIENCE, ENGINEERING & HUMANITIES (ICIASEH-2020),* 2020.

[18] C.-W. Chen, S.-Y. Hsiao, C.-Y. Chen, H.-W. Kang, Z.-Y. Huang, and H.-W. Lin, "Optical properties of organometal halide perovskite thin films and general device structure design rules for perovskite single and tandem solar cells," *Journal of Materials Chemistry A,* vol. 3, no. 17, pp. 9152-9159, 2015, doi: https://doi.org/10.1039/C4TA05237D.

[19] Y. Wang, *Investigation of perovskite-CIGSe tandem solar cells*. Technische Universitaet Berlin (Germany), 2019.

[20] M. Attygalle and D. Ratnasinghe, "Modelling of CdTe/Si Tandem Solar Cell With a Magnesium Doped Zinc Oxide Window Layer and Introducing a Surface Defects Layer Between Emitter/Absorber," in *Proceedings of the 6th International Conference on Multidisciplinary Approaches (iCMA)*, 2019.

[21] N. Touafek and R. Mahamdi, "Excess defects at the CdS/CIGS interface solar cells," *Chalcogenide Letters,* vol. 11, no. 11, pp. 589-596, 2014.

[22] S. Ouédraogo, F. Zougmoré, and J. Ndjaka, "Computational analysis of the effect of the surface defect layer (SDL) properties on Cu (In, Ga) Se2-based solar cell performances," *Journal of Physics and Chemistry of Solids,* vol. 75, no. 5, pp. 688-695, 2014, doi: https://doi.org/10.1016/j.jpcs.2014.01.010.

[23] S. Ouédraogo, F. Zougmoré, and J. Ndjaka, "Numerical analysis of copper-indium-gallium-diselenide-based solar cells by SCAPS-1D," *International Journal of Photoenergy,* vol. 2013, 2013, doi: https://doi.org/10.1155/2013/421076.

[24] C.-S. Jiang, F. Hasoon, H. Moutinho, H. Al-Thani, M. Romero, and M. Al-Jassim, "Direct evidence of a buried homojunction in Cu (In, Ga) Se 2 solar cells," *Applied Physics Letters,* vol. 82, no. 1, pp. 127-129, 2003, doi: https://doi.org/10.1063/1.1534417.

[25] W. Shockley and W. Read Jr, "Statistics of the recombinations of holes and electrons," *Physical review,* vol. 87, no. 5, p. 835, 1952, doi: https://doi.org/10.1103/PhysRev.87.835.

[26] R. N. Hall, "Electron-hole recombination in germanium," *Physical review,* vol. 87, no. 2, p. 387, 1952, doi: https://doi.org/10.1103/PhysRev.87.387.

[27] D. Ratnasinghe and M. Attygalle, "Numerical Investigation of the Best Efficient Tandem Solar Cell Structures Using the Base Cell Models of MZO/CdTe and CdS/CIGS Cell Structures," *IJMS,* vol. 6, no. 1, pp. 20-24, 2019, doi: http://doi.org/10.4038/ijms.v6i1.88.